

Cluster Compounds

DOI: 10.1002/anie.200504600

Discovery of a Family of Isopolyoxotungstates $[\text{H}_4\text{W}_{19}\text{O}_{62}]^{6-}$ Encapsulating a $\{\text{WO}_6\}$ Moiety within a $\{\text{W}_{18}\}$ Dawson-like Cluster Cage***De-Liang Long,* Paul Kögerler, Alexis D. C. Parenty, John Fielden, and Leroy Cronin**

Polyoxotungstates are continuing to attract attention because of their appealing electronic and molecular properties that give rise to many applications in, for example, catalysis^[1] and materials science.^[2] Since their materials properties are intricately linked to their structural features, the creation of novel polyoxotungstate structural types remains a pressing challenge. However, the development of new structures has thus far mostly involved the integration of heteroanions or heterometals that support the tungstate-based frameworks.^[3] Only a few examples of basic types of isopolyoxotungstates are known, including $[\text{HW}_5\text{O}_{19}]^{7-}$,^[4] $[\text{W}_6\text{O}_{19}]^{2-}$,^[5]

[*] Dr. D.-L. Long, Dr. A. D. C. Parenty, Prof. Dr. L. Cronin
Department of Chemistry
The University of Glasgow
Glasgow, G12 8QQ (UK)
Fax: (+44) 141-330-4888
E-mail: longd@chem.gla.ac.uk
l.cronin@chem.gla.ac.uk

Dr. P. Kögerler, Dr. J. Fielden
Ames Laboratory and Department of Physics and Astronomy
Iowa State University
Ames, IA 50011 (USA)

[**] This work was supported by the EPSRC and the University of Glasgow.



Supporting information for this article is available on the WWW under <http://www.angewandte.org> or from the author.

$[\text{H}_3\text{W}_6\text{O}_{22}]^{5-}$,^[6] $[\text{W}_7\text{O}_{24}]^{6-}$,^[7] $[\text{W}_{10}\text{O}_{32}]^{4-}$,^[8] $[\text{H}_4\text{W}_{11}\text{O}_{38}]^{6-}$,^[9] $[\text{H}_2\text{W}_{12}\text{O}_{40}]^{6-}$, $[\text{H}_2\text{W}_{12}\text{O}_{42}]^{10-}$, and $[\text{W}_{24}\text{O}_{84}]^{24-}$.^[10] The synthesis of fundamentally new isopolyoxotungstates, which may subsequently be used as building blocks in constructing larger architectures or networks, therefore requires new strategies that exploit supramolecular interactions during the construction of the cluster architecture. In this context we recently explored the use of larger, flexible organic cations that allowed us to isolate new cluster structures, for example, the isopolyoxomolybdate $[\text{H}_2\text{Mo}_{16}\text{O}_{52}]^{10-}$ ^[11] using protonated hexamethylenetetramine, which encapsulates this unit in solution, thereby limiting its reorganization to simpler structure types. We extended this strategy to tungstate-based systems by using protonated triethanolamine (TEAH^+) as cations at around pH 2 and isolated the isopolyoxotungstate $[\text{H}_{12}\text{W}_{36}\text{O}_{120}]^{12-}$, which can be thought of as an inorganic “crown ether”.^[12] Notably, the same reaction system at lower pH values (around 1) yields a fundamentally new type of isopolyoxotungstate $[\text{H}_4\text{W}_{19}\text{O}_{62}]^{6-}$ (**1a**), which was isolated as its salt $(\text{TEAH})_6[\text{H}_4\text{W}_{19}\text{O}_{62}]$ (**1**).

Compound **1** forms after refluxing a solution of sodium tungstate and TEAH^+ at pH 0.8 for more than three days, during which time the solution gradually changes from colorless to pale green. In the absence of the bulky organic TEAH^+ cations, under otherwise identical reaction conditions, only the well-known $[\text{W}_{10}\text{O}_{32}]^{4-}$ cluster compound forms, which implies the existence of a crucial cation effect.^[13] Although crystals of **1** were of poor quality, which meant that the cluster oxido positions and the TEAH^+ cations could not be well resolved because of disorder,^[14] the metal skeleton of 19 W centers is clearly resolved and resembles that of a Dawson-type $\{\text{W}_{18}\}$ cage (realized for instance as $[\text{W}_{18}\text{O}_{54}(\text{PO}_4)_2]^{6-}$)^[15] featuring an additional W center located in the center of the cluster and the absence of the two heteroatoms typically associated with Dawson-type clusters.

Analysis of **1** by ^{183}W NMR spectroscopy in aqueous solution shows three groups of W centers, which correspond to a single tungsten center and two types of tungsten centers typically found in a Dawson-type cluster sphere (consisting of six “cap” and twelve “belt” W atoms). Furthermore, recrystallization of **1** in water yields a new crystal form **1'**,^[14] which has cubic morphology and composition $(\text{TEAH})_6[\text{H}_4\text{W}_{19}\text{O}_{62}] \cdot 6\text{H}_2\text{O}$. The vastly improved crystal quality led to a better resolved structure with minimal disorder of the central WO_6 environment and the positions of the capping W centers.^[14] Thus, $[\text{H}_4\text{W}_{19}\text{O}_{62}]^{6-}$ represents the first example of an isopolyanion adopting a Dawson-type heteropolyanion framework structure.^[15,16]

The disorder pattern found in the structures of **1** (and **1'**) implies that different isomers of **1a** cocrystallize in **1** (and **1'**) which cannot be resolved in the presence of water as a solvent and TEAH^+ cations. To explore the $\{\text{W}_{19}\}$ cluster type fully, cation exchange and transformation of the clusters into organic solvent were performed by redissolving **1** in water and precipitating the $\{\text{W}_{19}\}$ cluster with *n*-tetrapropylammonium (Pr_4N^+) and recrystallizing the resulting precipitate from acetonitrile. Two isomers $(\text{Pr}_4\text{N})_6[\text{H}_4\text{W}_{19}\text{O}_{62}] \cdot 6\text{CH}_3\text{CN}$ (**2**) and $(\text{Pr}_4\text{N})_6[\text{H}_4\text{W}_{19}\text{O}_{62}] \cdot 3\text{CH}_3\text{CN}$ (**3**) were successfully

obtained as crystalline solids and were fully characterized by single-crystal X-ray diffraction.^[14] Compound **2** crystallizes in a monoclinic system (space group $C2$) with two crystallographically independent cluster halves in the asymmetric unit, where both complete clusters consist of a Dawson-type $\{\text{W}_{18}\}$ cage and an additional central W site that lies on crystallographic C_2 axes. Figure 1 shows one of the two complete

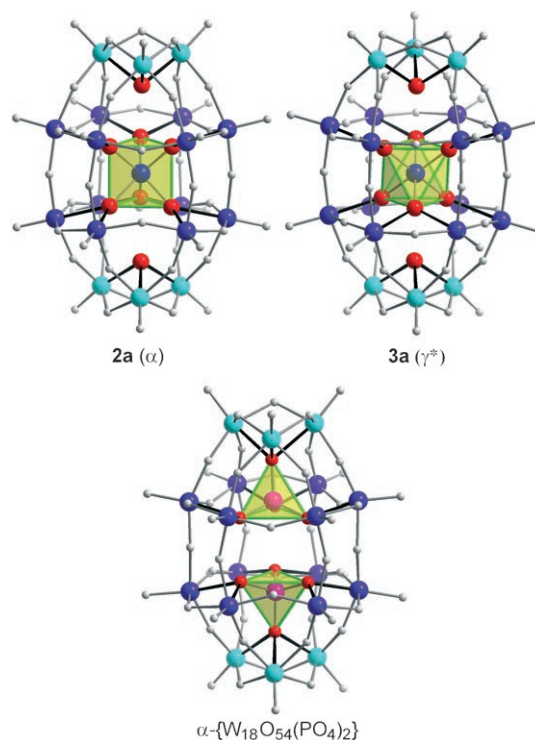


Figure 1. Structural representation of the $\{\text{W}_{19}\}$ isopolyoxotungstate isomers **2a** and **3a** as well as the phosphate-based Dawson anion $\alpha\text{-}[\text{W}_{18}\text{O}_{54}(\text{PO}_4)_2]^{6-}$ ^[15] for comparison. The central XO_n anion templates are emphasized as green/transparent yellow polyhedra (a trigonal WO_6 prism in **2a**, a WO_6 octahedron in **3a**, two PO_4 tetrahedra in $\alpha\text{-}[\text{W}_{18}\text{O}_{54}(\text{PO}_4)_2]^{6-}$). The eight oxido ligands in each cluster that span the two tetrahedral areas (empty in **2a** and **3a**, occupied by P in the phosphate Dawson structure) are shown in red; their bonds to W centers are emphasized in black. W: blue (“belt” positions and central position), light blue (“cap” positions), O: light gray, P: pink.

clusters (**2a**), defined as the D_{3h} -symmetric α isomer of the new isopolyoxotungstate $[\text{H}_4\text{W}_{19}\text{O}_{62}]^{6-}$ family. Cluster **2a** consists of the $\{\text{W}_{18}\text{O}_{54}\}$ cage framework and interior oxido ligands of the conventional Dawson cluster anion $\alpha\text{-}[\text{W}_{18}\text{O}_{54}(\text{XO}_4)_2]^{n-}$ ($\text{X} = \text{P}, \text{S}$)^[15] but, in contrast to the classical Dawson structure, the two tetrahedral XO_4^{n-} heteroanions are replaced by a trigonal-prismatic WO_6^{6-} anion and two μ_3 -oxido ligands (partially protonated, see below), each of which bridges the capping $\{\text{W}_3\}$ triangle from the inside of the cluster with an average $\text{W}\text{--}\text{O}$ bond length of 2.23(3) Å. To the best of our knowledge, this is the first observation in polyoxotungstates of a $\{\text{WO}_6\}$ unit in which the W center adopts a trigonal-prismatic coordination environment with all $\text{W}\text{--}\text{O}$ bond lengths virtually identical (1.96(3) Å)—in all previous examples the $\{\text{WO}_6\}$ units typically display octahedral geometries

with one or two short terminal W=O bonds and some longer W-(μ -O) bonds. Two tetrahedral “voids” exist in **2a** at the positions that are typically occupied by the heteroatoms in conventional Dawson cluster anions α -[W₁₈O₅₄(XO₄)₂]ⁿ⁻. Two of the four oxido ions that define each tetrahedral “void” are protonated and form H-bonds with the other two ions, which is similar to the corresponding situations inside the Keggin cluster [H₂W₁₂O₄₀]⁶⁻[17] and the semivacant Dawson polyoxotungstate [Ce{P(H₄)W₁₇O₆₁}]¹⁹⁻[18]. This protonation assignment is supported by ¹H NMR measurements, elemental analyses, bond valence sum analysis, and crystal structure determinations, which showed only six Pr₄N⁺ counteranions per cluster in **2**. Interestingly, **2a** bears some resemblance to the {W₁₈} type cluster α -[H₂W₁₈NaO₅₆F₆]⁷⁻ previously reported by Baker and co-workers[19] in which the central template [NaF₆]⁵⁻ also displays a trigonal prismatic configuration with six Na-F bond lengths in the range from 2.17 to 2.32 Å, which are significantly longer than those of the corresponding W-O bond lengths of the central {WO₆}⁶⁻ unit in **2a**. The F-W bonds (ca. 2.22 Å) are much shorter than the corresponding O-W bonds (ca. 2.42 Å) in **2a**. Bearing the geometric similarity of these two structures in mind, we have carefully checked the position of the central W atom in **2a**. However, all evidence from structure refinement, spectra, and chemical analyses unambiguously confirmed the central position as a tungsten center. In addition we have measured the cold-spray mass spectra of an acetonitrile solution of **2** and **3**, which clearly showed the intact cluster in the gas phase: {(Pr₄N)₅-**2a**}¹⁻ and {(Pr₄N)₅-**3a**}¹⁻ were observed at *m/z* 5420 and could be unambiguously assigned by comparison to the expected isotopic envelope.

Compound **3** crystallizes in an orthorhombic system (space group *Pccn*)^[14] and contains the [H₄W₁₉O₆₂]⁶⁻ cluster **3a** as the centrosymmetric γ^* isomer with *D*_{3d} symmetry (Figure 1). Cluster **3a** is based on the geometry of the {W₁₈O₅₄} cage framework and interior oxido ligands as found in the conventional Dawson cluster anion γ^* -[W₁₈O₅₄(SO₄)₂]⁴⁻[20]. Again, an additional W site is located at the center of the cluster and coordinates to six oxido ligands to form a central {WO₆} centrosymmetric template of octahedral geometry. As in **2a**, two further μ_3 -oxido ligands inside the cluster each bridge one of the capping {W₃} triangles with an average W-O bond length of 2.28(1) Å. All W-O bond lengths in the {WO₆} central template of **3a** are nearly identical (1.95(3) Å), and such a {WO₆} octahedral geometry is also the first observation of this kind in polyoxotungstates. Two tetrahedral “voids” similar to those in **2a** are occupied by two protons each and this is confirmed by ¹H NMR results. Unlike the chemical shift values found in the ¹H NMR spectrum of the Keggin cluster [H₂W₁₂O₄₀]⁶⁻, which only shows one peak at around 6.0 ppm because of the inner regular tetrahedral O₄ environment (with O...O distances of approximately 2.90 Å), several peaks corresponding to the four protons present within the clusters **2** and **3** are found in the range 4.7–8.1 ppm (and all these peaks integrate to about 4 protons per cluster). This observation can be explained by the trigonal pyramidal (nontetrahedral) environment. In **2**, the average base length (O...O) of the pyramid is 2.61(5) Å, while the side length is 2.85(2) Å. In **3**, these two values are

2.73(3) and 2.96(2) Å. Strong hydrogen bonding (indicated by short O...O separations in **2** and **3**) means that the protons will be observed at lower chemical shifts (e.g. δ = 4.7 ppm), and, since the local symmetry is lowered, the four protons are not equivalent. In the ¹H NMR spectrum of **1** in D₂O, only aliphatic protons (-CH₂- in TEAH⁺) are resolved as the protons present in the clusters were not observed owing to rapid exchange with solvent, which is similar to the case in semivacant Dawson polyoxotungstate [Ce{P(H₄)W₁₇O₆₁}]¹⁹⁻[18]. However, we were able to measure a ¹H NMR spectrum of **1** in DMSO which shows several peaks at δ = 8.01, 7.23, 5.74, 5.27, 4.66, 4.45, and 4.0 ppm. As **1** is not soluble in CD₃CN, any comparison of ¹H NMR spectra for **1**, **2**, and **3** is purely qualitative; this is because of the possibility of several protonation sites and uncertainty about the population at a given site. However, it is notable that the same types of proton environment associated with pure isomers **2** and **3** all have corresponding shifts found in **1**, which contains the isomers found in **2** and **3**.

The difference between the {W₁₉} isomers **2a** and **3a** concerns the {W₁₈O₅₄} cage and central template {WO₆} geometries. Topological analysis indicates that, besides **2a** and **3a**, other isomers are possible: the [H₄W₁₉O₆₂]⁶⁻ family consists of six isomers that are also observed for the conventional Dawson anions [W₁₈O₅₄(XO₄)₂]ⁿ⁻ (X = P, S, etc.)^[15,20] that is, the same {W₁₈O₅₄} cage variations and interior bridging oxido group orientations are present; we therefore adopt the same isomer designations (α , α^* , β , β^* , γ , γ^*)^[21]. The α , β , and γ isomers all contain the trigonal prismatic {WO₆} central unit (*D*_{3h}), whereas the α^* , β^* , and γ^* isomers contain a centrosymmetric octahedral {WO₆} central unit (*D*_{3d}). α , β^* , and γ isomers all form a *D*_{3h}-symmetric {W₁₈} cage whereas the α^* , β , and γ^* isomers all form a *D*_{3d}-symmetric {W₁₈} cage. As the point groups of the {W₁₈} cages and the {WO₆} central units match, the complete α and γ cluster isomers adopt *D*_{3h} symmetry, whereas the α^* and γ^* cluster isomers adopt *D*_{3d} symmetry. The symmetry mismatch for the {W₁₈} cages and central {WO₆} units in both β and β^* isomers reduces their overall symmetry to *C*_{3v}. Therefore, the comparison between the {W₁₈} Dawson and the {W₁₉} structure types is strengthened not only by their framework topology, but also by the fact that the 18 tungsten centers of the {W₁₈} cages of the corresponding α and γ^* isomers occupy exactly the same positions in both structure types within an error margin of 0.2 Å.

Planar projections (Schlegel diagrams) were constructed to understand the connectivity of the Dawson-type {W₁₈} and our {W₁₉} frameworks better and to examine the similarity between the two.^[22] Schlegel diagrams can be used for the Dawson-like clusters to describe the {W₁₈} cage frameworks in which each link represents a bridging oxido ligand between W atoms. Therefore in the *D*_{3h}-symmetric systems (Figure 2a), the edges of the outmost and innermost triangles (capping {W₃} groups) are parallel, whereas in the *D*_{3d}-symmetric systems (Figure 2b), these two triangles are inverted with respect to each other. These two configurations, combined with the orientations and geometries of the central {WO₆} units as described above, produce planar projections of all six isomers. Figure 2 demonstrates the α isomer **2a** and γ^* isomer

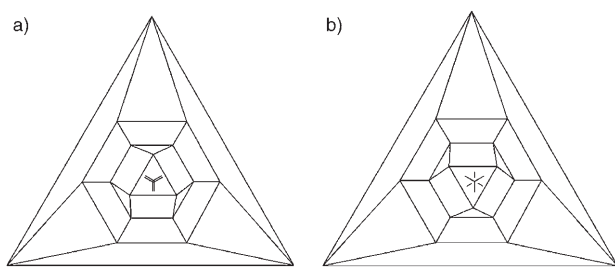
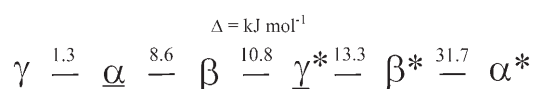


Figure 2. Schlegel diagrams of the $\{W_{18}\}$ cage structures together with the central WO_6 units shown as eclipsed (trigonal prismatic) and staggered lines (octahedral). a) α isomer and b) γ^* isomer. Other isomers can be deduced in the following ways: β isomer: the $\{W_{18}\}$ cage in (b) plus WO_6 unit in (a); γ isomer: α isomer in (a) with the WO_6 unit turned by 60° along the main C_3 axis; α^* isomer: γ^* isomer in (b) with the WO_6 unit turned by 60° along the main C_3 axis; β^* isomer: the cage in (a) plus WO_6 unit in (b).

3a. Other representations of the remaining four isomers can be derived from these projections.

To examine the principal relation of these isomers further, we scaled the stabilities of all six isomers by their relative energies from density functional theory calculations on the cluster anions (Scheme 1).^[23] These calculations, performed



Scheme 1. Scheme of the relative energies of the cluster isomers as calculated by DFT. The experimentally characterized cluster isomers **2a** (α) and **3a** (γ^*) are underlined.

on geometrically relaxed isolated cluster geometries in the gas phase, suggest that the D_{3h} -symmetric α isomer is more stable than the D_{3d} -symmetric γ^* isomer. The γ and γ^* structures are only separated by 21 kJ mol^{-1} , whereas the α -to- α^* energy difference is over three times larger (64 kJ mol^{-1}). It is important to note that these relative energies only reflect the differing connectivities of the idealized isomer geometries; the actual formation and interconversion of individual isomers is subject to a large set of bulk phase parameters. Having isolated pure α and γ^* isomers, we investigated the stability of these compounds by using differential scanning calorimetry (DSC). The DSC trace for compound **2** shows a broad endothermic peak starting at 315°C , possibly resulting from the reduction of the cluster by the organic cations, as suggested by the color change to blue observed at this temperature. Compound **3** also shows this feature, as well as a small endothermic peak immediately followed by an exothermic peak ($291\text{--}298^\circ\text{C}$). These latter irreversible processes are possibly due to either a rearrangement/decomposition in the cluster shell or associated cations; however, solvent effects have been ruled out.^[24]

In summary, we have demonstrated that it is possible to isolate isopolyoxotungstate clusters that are structural analogues of heteropolyacids, in this case, of the Dawson structural archetype. The isolation of two of the six isomers that make up this new family, along with the chemical,

thermogravimetric, and theoretical analysis, demonstrates interesting features related to the inclusion of the $[WO_6]^{6-}$ anion template. Furthermore, the stabilization of the $[WO_6]$ moiety in a trigonal prismatic coordination environment is unprecedented in polyoxotungstate chemistry. Future work will include exploring the potential redox chemistry, photochemistry, and acidic nature of the clusters to compare their physical properties directly with the classical Dawson clusters. In addition, the inclusion of the metal-based octahedra may allow control of the formation of clusters using other $\{MO_6\}$ or $\{MX_6\}$ units as templates.

Experimental Section

1: Triethanolamine hydrochloride (14.0 g, 75.4 mmol) and $Na_2WO_4 \cdot 2H_2O$ (13.0 g, 39.4 mmol) were dissolved in water (80 mL). Hydrochloric acid (6M) was added with stirring to adjust the pH to 1.2. The solution was then heated at reflux with stirring for 3 days. After the solution was cooled to room temperature, pale green needles crystallized over 2 days; these were then filtered, washed with ethanol, and dried in vacuum (3.8 g, 34% yield). IR (KBr): $\tilde{\nu} = 3434, 1631, 1446, 1400, 1258, 1202, 1091, 1060, 1027, 961, 767, 614 \text{ cm}^{-1}$; elemental analysis (%) calcd for $C_{36}H_{100}N_6O_{80}W_{19}$: C 8.02, H 1.87, N 1.56, W 64.8; found: C 8.04, H 1.84, N 1.54, W 64.5. 1H NMR (400 MHz, DMSO): TEAH⁺ was observed at $\delta = 8.48$ NH (6H), 5.27 OH (18H), 3.79 CH_2 (36H), 3.4 ppm CH_2 (36H); $[H_4W_{19}O_{62}]^{6-}$ at $\delta = 8.01, 7.23, 5.74, 5.27, 4.66, 4.45, 4.0$ ppm, integrated to ca. 3.2. ^{183}W NMR (16.668 MHz, D_2O , Na_2WO_4): three sets of resonances reflecting the presence of multiple isomers centered at $\delta = -115, -143, -165$ ppm which can be assigned to the central $\{W_1\}$, $\{W_{12}\}$ belt, and $\{W_6\}$ caps on the basis of Löwdin charge analysis from the DFT calculations. Recrystallization of **1** in water give pale green cubic crystals of $(TEAH)_6[H_4W_{19}O_{62}] \cdot 6H_2O$ (**1'**).

2 and 3: Freshly prepared compound **1** (2.0 g, 0.37 mmol) was dissolved in water (80 mL) with stirring. Pr_4NBr (2.2 g) in water (50 mL) was added and the mixture was stirred for a further 10 minutes. The light precipitate was centrifuged, washed with water, ethanol, and diethyl ether, and dried in vacuum. The dried sample was then extracted with acetonitrile (140 mL). Evaporation of the extract yielded colorless lath crystals of **2** (0.68 g, 33%) and very light cream yellow polyhedral crystals of **3** (0.45 g, 21%), along with some noncrystalline powder of other possible isomers on the glass wall with elemental analyses close to those calculated for the composition $C_{72}H_{172}N_6O_{62}W_{19}$. **2** and **3** were separated manually, and recrystallization of **2** and **3** helped to purify them further. **2** loses solvent and decays in minutes after being taken from the solution, whereas **3** is stable with included solvent molecules and is still suitable for X-ray structure determination several days after being taken from the solution. Analysis of **2**: 1H NMR (400 MHz, CD_3CN): $\delta = 1.00$ - CH_3 (72H), 1.7 - CH_2 - (48H), 3.1 - CH_2 - (48H), 4.5 H (0.8H), 7.6 H (0.7H), 8.1 ppm H (2.5H); IR (KBr): $\tilde{\nu} = 3542, 2970, 2881, 1627, 1387, 1324, 1158, 1024, 961, 876, 799 \text{ cm}^{-1}$; elemental analysis (%) calcd for $C_{72}H_{172}N_6O_{62}W_{19}$ (after losing solvated acetonitrile and vacuum drying): C 15.42, H 3.09, N 1.50, W 62.3; found: C 15.30, H 2.95, N 1.50, W 61.8. Analysis of **3**: 1H NMR (400 MHz, CD_3CN): $\delta = 1.00$ - CH_3 (72H), 1.7 - CH_2 - (48H), 3.1 - CH_2 - (48H), 4.7 H (2.2H), 6.7 H (0.5H), 7.6 H (0.8H), 8.1 H (0.5H); IR (KBr): $\tilde{\nu} = 3410, 2975, 2881, 1484, 1385, 1013, 962, 815 \text{ cm}^{-1}$; elemental analysis (%) calcd for $C_{78}H_{181}N_9O_{62}W_{19}$: C 16.35, H 3.18, N 2.20; found: C 16.30, H 3.17, N 2.23.

$(Pr_4N)_4[W_{10}O_{32}] \cdot CH_3CN$ (in the absence of TEA): $Na_2WO_4 \cdot 2H_2O$ (3.3 g, 10 mmol) was dissolved in water (50 mL). The pH of the solution was adjusted to 1.2 using hydrochloric acid (6M), and the solution was heated at reflux for 3 days. After the solution was cooled to room temperature, a solution of Pr_4NBr (1.7 g) in water (30 mL)

was added and the precipitated product was collected, washed with ethanol, dried in vacuum, and recrystallized from CH₃CN (2.8 g, 89% yield, based on W). IR (KBr): $\tilde{\nu}$ = 2976, 1681, 1629, 1474, 1380, 1325, 1105, 1041, 961, 894, 804, 589 cm⁻¹; elemental analysis (%) calcd for C₃₀H₁₁₅N₅O₃₂W₁₀: C 19.14, H 3.70, N 2.23, W 58.6; found: C 19.01, H 3.47, N 2.15, W 57.9.

Received: December 28, 2005

Revised: April 25, 2006

Published online: June 28, 2006

Keywords: cluster compounds · electronic structure · polyoxometalates · self-assembly · tungsten

- [1] V. M. Hultgren, B. P. Timko, A. M. Bond, W. R. Jackson, A. G. Wedd, *J. Am. Chem. Soc.* **2003**, *125*, 10133; W. B. Kim, T. Voitl, G. J. Rodriguez-Rivera, S. T. Evans, J. A. Dumesic, *Angew. Chem.* **2005**, *117*, 788; *Angew. Chem. Int. Ed.* **2005**, *44*, 778.
- [2] K. F. Aguey-Zinsou, P. V. Bernhardt, U. Kappler, A. G. McEwan, *J. Am. Chem. Soc.* **2003**, *125*, 530; D. A. Judd, J. H. Nettles, N. Nevins, J. P. Snyder, D. C. Liotta, J. Tang, J. Ermolieff, R. F. Schinazi, C. L. Hill, *J. Am. Chem. Soc.* **2001**, *123*, 886; M. T. Pope, A. Müller, *Angew. Chem.* **1991**, *103*, 56; *Angew. Chem. Int. Ed. Engl.* **1991**, *30*, 34; F. Ogliaro, S. P. de Visser, S. Cohen, P. K. Sharma, S. Shaik, *J. Am. Chem. Soc.* **2002**, *124*, 2806; T.-R. Zhang, W. Feng, R. Lu, C.-Y. Bao, T.-J. Li, Y.-Y. Zhao, J. N. Yao, *J. Solid State Chem.* **2002**, *166*, 259; T. Yamase, *Chem. Rev.* **1998**, *98*, 307.
- [3] For recent examples of novel polyanion structures, see for example: a) Y. Jeannin, *C. R. Chim.* **2004**, *7*, 1235; b) W. Yang, C. Lu, H. Zhuang, *Inorg. Chem. Commun.* **2002**, *5*, 865; c) D. Drewes, G. Vollmer, B. Krebs, *Z. Anorg. Allg. Chem.* **2004**, *630*, 2573; d) U. Kortz, M. G. Savelieff, B. S. Bassil, M. H. Dickman, *Angew. Chem.* **2001**, *113*, 3488; *Angew. Chem. Int. Ed.* **2001**, *40*, 3384; e) B. S. Bassil, S. Nellutla, U. Kortz, A. C. Stowe, J. van Tol, N. S. Dalal, B. Keita, L. Nadjo, *Inorg. Chem.* **2005**, *44*, 2659.
- [4] J. Fuchs, R. Palm, H. Hartl, *Angew. Chem.* **1996**, *108*, 2820; *Angew. Chem. Int. Ed. Engl.* **1996**, *35*, 2651.
- [5] R. Bhattacharyya, S. Biswas, J. Armstrong, E. M. Holt, *Inorg. Chem.* **1989**, *28*, 4297.
- [6] H. Hartl, R. Palm, J. Fuchs, *Angew. Chem.* **1993**, *105*, 1545; *Angew. Chem. Int. Ed. Engl.* **1993**, *32*, 1492.
- [7] K. G. Burtseva, T. S. Chernaya, M. I. Sirota, *Dokl. Akad. Nauk* **1978**, *243*, 104; J. Fuchs, E. P. Flindt, *Z. Naturforsch. B* **1979**, *34*, 412.
- [8] Y. Sasaki, T. Yamase, Y. Ohashi, Y. Sasada, *Bull. Chem. Soc. Jpn.* **1987**, *60*, 4285.
- [9] T. Lehmann, J. Z. Fuchs, *Z. Naturforsch. B* **1988**, *43*, 89.
- [10] I. Brüdgam, J. Fuchs, H. Hartl, R. Palm, *Angew. Chem.* **1998**, *110*, 2814; *Angew. Chem. Int. Ed.* **1998**, *37*, 2668, and references therein.
- [11] D.-L. Long, P. Kögerler, L. J. Farrugia, L. Cronin, *Angew. Chem.* **2003**, *115*, 4312; *Angew. Chem. Int. Ed.* **2003**, *42*, 4180; D.-L. Long, P. Kögerler, L. J. Farrugia, L. Cronin, *Dalton Trans.* **2005**, 1372.
- [12] D.-L. Long, H. Abbas, P. Kögerler, L. Cronin, *J. Am. Chem. Soc.* **2004**, *126*, 13880; D.-L. Long, O. Brücher, C. Streb, L. Cronin, *Dalton Trans.* **2006**, 2852.
- [13] Crystal data and structure refinements for (Pr₄N)₄[W₁₀O₃₂]-CH₃CN: C₃₂H₁₁₈N₆O₃₂W₁₀, $M_r = 3178.02$ g mol⁻¹; triclinic, space group $P\bar{1}$, $a = 12.0974(4)$, $b = 13.9624(4)$, $c = 14.2581(4)$ Å, $\alpha = 70.213(2)^\circ$, $\beta = 75.129(2)^\circ$, $\gamma = 79.298(2)^\circ$, $V = 2177.26(11)$ Å³, $Z = 1$, $\rho = 2.424$ g cm⁻³, $\mu(\text{MoK}\alpha) = 13.22$ mm⁻¹, $F(000) = 1468$, 30461 reflections measured, 7663 unique ($R_{\text{int}} = 0.052$), 450 refined parameters, $R1 = 0.0372$, $wR2 = 0.0911$.
- [14] Crystal data and structure refinements for **1**: C₃₆H₁₀₀N₆O₈₀W₁₉, $M_r = 5390.13$ g mol⁻¹; triclinic, space group $P\bar{1}$, $a = 13.7245(10)$, $b = 13.9719(10)$, $c = 16.2396(9)$ Å, $\alpha = 86.865(5)^\circ$, $\beta = 74.245(4)^\circ$, $\gamma = 61.093(2)^\circ$, $V = 2612.8(3)$ Å³, $Z = 1$, $\rho = 3.426$ g cm⁻³, $\mu(\text{MoK}\alpha) = 20.92$ mm⁻¹, $F(000) = 2404$, 28808 reflections measured, 7231 unique ($R_{\text{int}} = 0.089$), 415 refined parameters, $R1 = 0.0667$, $wR2 = 0.2014$. **1'**: C₃₆H₁₁₂N₆O₈₆W₁₉, $M_r = 5498.47$ g mol⁻¹; trigonal, space group $R\bar{3}$, $a = 21.471(2)$, $c = 19.9668(12)$, $V = 7971.6(12)$ Å³, $Z = 3$, $\rho = 3.436$ g cm⁻³, $\mu(\text{MoK}\alpha) = 20.58$ mm⁻¹, $F(000) = 7392$, 7325 reflections measured, 2921 unique ($R_{\text{int}} = 0.065$), 239 refined parameters, $R1 = 0.0536$, $wR2 = 0.1172$. **2**: C₈₄H₁₉₀N₁₂O₆₂W₁₉, $M_r = 5853.63$ g mol⁻¹; monoclinic, space group $C2$, $a = 30.7860(4)$, $b = 15.3098(2)$, $c = 29.9306(4)$ Å, $\beta = 94.515(1)^\circ$, $V = 14063.3(3)$ Å³, $Z = 4$, $\rho = 2.765$ g cm⁻³, $\mu(\text{MoK}\alpha) = 15.551$ mm⁻¹, $F(000) = 10720$, 56613 reflections measured, 24330 unique ($R_{\text{int}} = 0.054$), 1412 refined parameters, $R1 = 0.0441$, $wR2 = 0.0709$. **3**: C₇₈H₁₈₁N₉O₆₂W₁₉, $M_r = 5730.47$ g mol⁻¹; orthorhombic, space group $Pccn$, $a = 22.4058(7)$, $b = 24.6486(9)$, $c = 25.2268(8)$ Å, $V = 13932.0(8)$ Å³, $Z = 4$, $\rho = 2.732$ g cm⁻³, $\mu(\text{MoK}\alpha) = 15.693$ mm⁻¹, $F(000) = 10456$, 241605 reflections measured, 13703 unique ($R_{\text{int}} = 0.068$), 737 refined parameters, $R1 = 0.0269$, $wR2 = 0.0671$. Crystal data for **3** were measured on a Bruker ApexII CCD diffractometer by using MoK α radiation ($\lambda = 0.71073$ Å) at 100(2) K. For all other compounds, crystal data were measured on a Nonius Kappa CCD diffractometer by using MoK α radiation ($\lambda = 0.71073$ Å) at 150(2) K. CCDC 292393–292397 ((Pr₄N)₄[W₁₀O₃₂]-CH₃CN, **1**, **1'**, **2**, and **3**, respectively) contain the supplementary crystallographic data for this paper. These data can be obtained free of charge from The Cambridge Crystallographic Data Centre via www.ccdc.cam.ac.uk/data_request/cif.
- [15] B. Dawson, *Acta Crystallogr.* **1953**, *6*, 113; M. Holscher, U. Englert, B. Zibrowius, W. F. Holderich, *Angew. Chem.* **1994**, *106*, 2552; *Angew. Chem. Int. Ed. Engl.* **1994**, *33*, 2491.
- [16] For nonconventional Dawson-like cluster compounds, see for examples: Y. Ozawa, Y. Sasaki, *Chem. Lett.* **1987**, 923; Y. Jeannin, J. Martin-Frere, *Inorg. Chem.* **1979**, *18*, 3010; U. Kortz, M. T. Pope, *Inorg. Chem.* **1994**, *33*, 5645. D.-L. Long, P. Kögerler, L. Cronin, *Angew. Chem.* **2004**, *116*, 1853; *Angew. Chem. Int. Ed.* **2004**, *43*, 1817; D.-L. Long, H. Abbas, P. Kögerler, L. Cronin, *Angew. Chem.* **2005**, *117*, 3481; *Angew. Chem. Int. Ed.* **2005**, *44*, 3415. All clusters contain heteroelements.
- [17] M. T. Pope, G. M. Varga, Jr., *Chem. Commun.* **1966**, 653; J. J. Hastings, O. W. Howarth, *J. Chem. Soc. Dalton Trans.* **1992**, 209.
- [18] N. Belai, M. H. Dickman, M. T. Pope, R. Constant, B. Keita, I.-M. Mbomekalle, L. Nadjo, *Inorg. Chem.* **2005**, *44*, 169.
- [19] T. L. Jorris, M. Kozik, L. C. W. Baker, *Inorg. Chem.* **1990**, *29*, 4584.
- [20] P. J. S. Richardt, R. W. Gable, A. M. Bond, A. G. Wedd, *Inorg. Chem.* **2001**, *40*, 703.
- [21] R. Contant, R. Thouvenot, *Inorg. Chim. Acta* **1993**, *212*, 41.
- [22] A. L. Loeb, *Space Structures—Their Harmony and Counterpoint*, Addison-Wesley, London, **1976**, p. 45.
- [23] Density functional theory calculations (including Löwdin and Mulliken population analysis) with the TURBOMOLE 5.7 package (O. Treutler, R. Ahlrichs, *J. Chem. Phys.* **1995**, *102*, 346) employed TZVP basis sets and hybrid B3-LYP exchange-correlation functionals. Equilibrated structures were obtained from free geometry optimizations starting with crystallographic data (α and γ^*) and with modeled geometries derived from these structures (α^* , β , β^* , γ). In both cases, proton positions were added by modeling and allowed to vary without symmetry restrictions in the course of the geometry optimization. The resulting optimized structures were found to be slightly expanded (owing to coulomb repulsion in the absence of countercharges). Calculated dipole moments: α : 0.538, α^* :

1.1352, β : 0.438, β^* : 1.034, γ : 0.998, γ^* : 0.976 debye. For a review on ab initio calculations on polyoxotungstates, see also J. M. Poblet, X. López, C. Bo, *Chem. Soc. Rev.* **2003**, 32, 297.

- [24] The two inherently coupled processes have been reproduced for multiple samples on two different DSC instruments. Changes in the heating rate do not change the relative peak positions or integrated energies associated with each of the processes; the process at 291–298 °C cannot be due to solvent loss since a simultaneous DSC/TGA experiment demonstrates total solvent loss below 250 °C.